the plant journal

SEB SOCIETY FOR EXPERIMENTAL BIOLOGY

The Plant Journal (2019) doi: 10.1111/tpj.14553

Maximizing leaf carbon gain in varying saline conditions: An optimization model with dynamic mesophyll conductance

Rangjian Qiu[1,2,*] and Gabriel G. Katul[2,3]

[1]*Collaborative Innovation Center on Forecast and Evaluation of Meteorological Disasters, Jiangsu Key Laboratory of Agricultural Meteorology, School of Applied Meteorology, Nanjing University of Information Science and Technology, Nanjing 210044, China,*

[2]*Nicholas School of the Environment, Duke University, Durham, NC 27708, USA, and*

[3]*Department of Civil and Environmental Engineering, Duke University, Durham, NC 27708, USA*

Received 22 July 2019; revised 10 September 2019; accepted 20 September 2019.

*For correspondence (e-mail qiurj@nuist.edu.cn).

SUMMARY

While the adverse effects of elevated salinity levels on leaf gas exchange in many crops are not in dispute, representing such effects on leaf photosynthetic rates (*A*) continues to draw research attention. Here, an optimization model for stomatal conductance (g_c) that maximizes *A* while accounting for mesophyll conductance (g_m) was used to interpret new leaf gas exchange measurements collected for five irrigation water salinity levels. A function between chloroplastic CO_2 concentration (c_c) and intercellular CO_2 concentration (c_i) modified by salinity stress to estimate g_m was proposed. Results showed that with increased salinity, the estimated g_m and maximum photosynthetic capacity were both reduced, whereas the marginal water use efficiency λ increased linearly. Adjustments of g_m, λ and photosynthetic capacity were shown to be consistent with a large corpus of drought-stress experiments. The inferred model parameters were then used to evaluate the combined effects of elevated salinity and atmospheric CO_2 concentration (c_a) on leaf gas exchange. For a given salinity level, increasing c_a increased *A* linearly, but these increases were accompanied by mild reductions in g_c and transpiration. The c_a level needed to ameliorate *A* reductions due to increased salinity is also discussed using the aforementioned model calculations.

Keywords: *Capsicum annum* L, mesophyll conductance, osmotic pressure, photosynthetic impairment, salt stress, stomatal optimization.

INTRODUCTION

Irrigation is routinely used for maintaining and increasing food production worldwide. Irrigated agricultural lands produce 40–45% of the world's food, and almost 90% of the global water use is for irrigation (Döll and Siebert, 2002). However, water scarcity remains the major limiting factor on expansion of irrigated agriculture in many parts of the world, especially in arid and semi-arid regions. In these regions, reliance on crops that require recycled irrigation water (e.g. saline water) is becoming necessary, which has an appreciable feedback on productivity and increased salinity (Runyan and D'Odorico, 2010). In some areas, up to 1200–1400 mm of saline water with salinity levels ranging from 2.2 to 3.7 dS m^{-1} have been used to meet crop water requirements (Ben-Gal *et al.*, 2008). Unsurprisingly, irrigation with high saline water does have adverse impacts on crop productivity, and its representation in mathematical models continues to draw research attention (Lycoskoufis *et al.*, 2005; Qiu *et al.*, 2017b).

High salinity induces both osmotic (short-term) and ionic (medium-to-long term) stresses that inhibit leaf photosynthetic (*A*) and transpiration (*E*) rates and stomatal conductance (g_c) at differing time scales as discussed elsewhere (Hsiao *et al.*, 1976; Morgan, 1984; Munns and Tester, 2008; Hossain and Dietz, 2016; Perri *et al.*, 2018). Under changing environmental conditions, stomata adjust their opening dynamically to govern CO_2 and H_2O diffusion into and out of leaves (Manzoni *et al.*, 2011). Open stomata result in liquid water molecules to experience a phase transition and escape into the atmosphere, while allowing for CO_2 molecules from the atmosphere to diffuse into the sub-stomatal (or internal) cavity. Under high salinity conditions, the short-term osmotic stress is assumed to act in a manner analogous to soil water stress and reduces g_c (Munns and Tester, 2008), which then leads to a decreased *E*.

Simultaneously, the diffusion of CO_2 from the atmosphere into the leaves is also reduced – though A may be less affected than E because plants have the ability to reduce their internal CO_2 partial pressure. Another limitation of osmotic stress is restricting CO_2 diffusion towards the chloroplast, where this pathway is commonly represented by the leaf mesophyll conductance (g_m). A large body of evidence indicates that g_m is not only finite and of similar magnitude to g_c (Flexas *et al.*, 2008), but is also reduced under soil water stress (Flexas *et al.*, 2002, 2004; Delfine *et al.*, 2005; Galmés *et al.*, 2007; Nadal and Flexas, 2018) and salinity stress (Delfine *et al.*, 1998, 1999; Centritto *et al.*, 2003; Loreto *et al.*, 2003). Hence, variation in g_m and g_c result in changes to A, and the sum of both stomatal and mesophyll resistances set a limit for the overall conductance experienced by CO_2 uptake under saline conditions (Flexas *et al.*, 2004; Volpe *et al.*, 2011; Perri *et al.*, 2019).

Experiments already report adverse effects of elevated salinity on gas exchanges (Chartzoulakis and Klapaki, 2000; Lycoskoufis *et al.*, 2005; Azuma *et al.*, 2010). However, what has resisted complete mathematical treatment is a phenomenological link between elevated salinity and reductions in A, E, g_m and g_c (Flowers *et al.*, 1977; Brugnoli and Lauteri, 1991; Steduto *et al.*, 2000), and this link frames the scope here. A stomatal optimization model for g_c is combined with a Farquhar photosynthesis model for C_3 plants and diffusional mass transport to interpret the effects of salt stress on leaf gas exchange experiments. Within the context of coupled hydrological-biogeochemical models, this approach assumes that stomatal aperture is adjusted so as to maximize A for a certain amount of saline water uptake (Volpe *et al.*, 2011). This hypothesis is compatible with the fact that uptaking saline water can cause measurable loss in carbon accumulation (Hsiao *et al.*, 1976; Morgan, 1984; Munns and Tester, 2008). The model proposed here revises earlier studies (Volpe *et al.*, 2011) by directly incorporating g_m and chloroplastic CO_2 concentration (c_c) using a proposed stress function discussed elsewhere (Dewar *et al.*, 2018; Perri *et al.*, 2019). The model provides a diagnostic of the relative impairment of the photosynthetic and hydraulic machinery using conventional gas exchange measurements. A literature review across a wide range of species is also conducted to assess similarities in impairment of the photosynthetic and hydraulic machinery of leaves due to salt- and drought stresses. Based on inferred parameters from gas exchange measurements, we also inquire as to whether and by how much elevated c_a might mitigate salinity stress in crops. The assessment of the magnitude of such compensation effect continues to be of interest in combined ecohydrological-climate change studies under saline conditions as well as phytoremediation efforts to reduce soil salinity in a fluctuating climate (Singh *et al.*, 2006; Bonan *et al.*, 2014; Jesus *et al.*, 2015).

RESULTS

Mathematical and modeling results

For steady-state conditions, the mass transfer of CO_2 and water vapor between leaves and the atmosphere are described by

$$A = g_c(c_a - c_i) = g_m(c_i - c_c), \tag{1}$$

and

$$E = 1.6 g_c \mathrm{VPD_L} = 1.6\ g_c(e_i - e_a), \tag{2}$$

where A is the leaf photosynthetic rate, E is leaf transpiration rate, g_c and g_m are the stomatal and mesophyll conductances to CO_2, respectively, c_a, c_i and c_c are the ambient, intercellular and chloroplastic CO_2 concentrations, respectively, and VPD_L is the vapor pressure deficit with respect to leaf temperature (T_L) representing the driving force for transpiration ($e_i - e_a$), where e_i and e_a are the intercellular and ambient water vapor concentrations, respectively. During photosynthesis, CO_2 is first transferred from the atmosphere into the sub-stomatal internal cavity through stomata, and then from there to the chloroplast through the leaf mesophyll (Flexas *et al.*, 2008). The effective conductance (g_{eff}) from the atmosphere to the chloroplast for photosynthesis can be determined from g_m and g_c using (Volpe *et al.*, 2011)

$$g_{eff} = \frac{g_c g_m}{g_c + g_m}, \tag{3}$$

so that the overall mass transfer to CO_2 can be expressed as

$$A = g_{eff}(c_a - c_c). \tag{4}$$

Here, the aerodynamic conductance g_a is assumed to be much larger than g_c or g_m as common when interpreting leaf-gas exchange measurements (described later). In typical gas exchange experiments, the measured g_a is higher than 2 mol m^{-2} sec^{-1}, which is at least one order of magnitude larger than g_m reported in the literature. When mitochondrial respiration (R_d) is small compared with A (neglecting R_d to derive the analytical solution), the Farquhar photosynthesis model for C_3 plants can be mathematically expressed as (Katul *et al.*, 2010; Launiainen *et al.*, 2011; Volpe *et al.*, 2011)

$$A = \frac{a_1(c_c - c_p)}{a_2 + c_c}, \tag{5}$$

where c_p is the CO_2 compensation point, a_1 and a_2 are parameters that depend on whether A is ribulose-1,5-bisphosphate carboxylase/oxygenase (hereafter Rubisco) or ribulose-1,5-biphosphate (hereafter RuBP) limited. For Rubisco limited A, a_1 is set to the maximum carboxylation

capacity (V_{cmax}) and $a_2 = K_c\,(1 + C_{oa}/K_o)$, where K_c and K_o are the Michaelis constants for CO_2 fixation and oxygen inhibition, respectively, and C_{oa} is the oxygen concentration in air (= 210 mmol mol^{-1}). The c_p, K_c and K_o have been shown to be T_L dependent (Ethier and Livingston, 2004; Sharkey *et al.*, 2007). For RuBP limited conditions, a_1 is set to the electron transport rate (J_{max}) and $a_2 = 2c_p$. When assuming steady-state conditions (i.e. every CO_2 molecule that enters through the leaf stomata from the atmosphere is assimilated), the Farquhar biochemical demand and atmospheric supply of CO_2 can be equated to yield

$$\frac{c_c}{c_a} = \frac{1}{2} + \frac{-a_1 - a_2 g_{eff} + \sqrt{\gamma_a}}{2c_a g_{eff}} \tag{6}$$

and

$$A = \frac{1}{2}\left[a_1 + (a_2 + c_a)g_{eff} - \sqrt{\gamma_a}\right], \tag{7}$$

where

$$\gamma_a = [a_1 + (a_2 - c_a)g_{eff}]^2 + 4g_{eff}\left(a_1 c_p + a_2 c_a g_{eff}\right). \tag{8}$$

To proceed further, a model for g_{eff} (or its two constituents g_c and g_m) is needed. Two approaches are now used and the mathematical results that emerge from implementing them are highlighted. One approach is sufficiently general and accommodates both RuBP and Rubisco limitations to *A*, whereas the second approach is only applicable to Rubisco limitations. Inherent to both approaches is the hypothesis that leaves autonomously maximize their carbon gain for a given amount of water by altering g_c (Givnish and Vermeij, 1976; Cowan and Farquhar, 1977; Cowan, 1978; Hari *et al.*, 1986; Katul *et al.*, 2009, 2010; Launiainen *et al.*, 2011; Manzoni *et al.*, 2011; Volpe *et al.*, 2011; Vico *et al.*, 2013). Mathematically, this hypothesis can be translated into a Hamiltonian to be maximized with respect to the independent variable g_c given as

$$H(g_c) = A - \lambda E = \frac{1}{2}\left[a_1 + (a_2 + c_a)g_{eff} - \sqrt{\gamma_a}\right] - 1.6\lambda g_c \mathrm{VPD_L}, \tag{9}$$

where λ is the cost of losing water in CO_2 units (i.e. linking the carbon and water economies of the plant) and is mathematically equivalent to the Lagrange multiplier (i.e. constant over time scales where g_c changes). Differentiating equation (9) with respect to g_c, setting $\partial H(g_c)/\partial g_c = 0$, and assuming $\partial g_m/\partial g_c = 0$ yields

This g_c or g_{eff} formulation is implicit and the analytical solution can be derived (not shown here). Combined with equations (3) and (10), the g_c can be solved and this solution is referred to as the non-linear optimization model.

To provide analytical results that can be discussed in general terms, a simpler solution is also presented that is restricted to Rubisco limitations. Expression $a_2 + c_c$ is written as $a_2 + (c_c/c_a)c_a = a_2 + sc_a$, where $s = c_c/c_a$. Inserting this expression into equation (5) yields

$$A = \frac{a_1\left(c_c - c_p\right)}{a_2 + sc_a}. \tag{11}$$

A linearization is now conducted that is only plausible when $a_2 > sc_a$ (i.e. Rubisco limitations on photosynthesis). For the case where $a_2 > sc_a$, small variations in *s* have a minor impact on $a_2 + sc_a$ and can be ignored. Thus, *s* is treated only as a constant in the expression $a_2 > sc_a$ resulting in a linear A–c_c biochemical demand function. For RuBP limitations on *A*, $a_2 = 2c_p < 80$ μmol mol^{-1}, but $c_c > 300$ μmol mol^{-1} is usually high so that $a_2 < c_c$ and the aforementioned approximation cannot hold. However, for Rubisco limitations on *A*, $a_2 > 550$ μmol mol^{-1} and $c_c < 300$ μmol mol^{-1} so that $a_2 > sc_a$, and treating *s* as a constant in the expression $a_2 + sc_a$ results in a linear biochemical demand function as expected in Rubisco limited *A* (Katul *et al.*, 2010; Volpe *et al.*, 2011). To be clear, *s* is treated as a constant only in the denominator of equation (11) but, everywhere else, it is allowed to vary. Upon combining equations (11) and (4),

$$\frac{c_c}{c_a} = \frac{a_1 c_p/c_a + g_{eff}(a_2 + sc_a)}{a_1 + g_{eff}(a_2 + sc_a)}, \tag{12}$$

and

$$A = \frac{a_1 g_{eff}\left(c_a - c_p\right)}{a_1 + g_{eff}(a_2 + sc_a)}. \tag{13}$$

Now equations (12) and (13) can be used in the Hamiltonian of equation (9) to yield:

$$H(g_c) = A - \lambda E = \frac{a_1 g_{eff}\left(c_a - c_p\right)}{a_1 + g_{eff}(a_2 + sc_a)} - \lambda\,(1.6\ g_c \mathrm{VPD_L}). \tag{14}$$

Upon differentiation with respect to g_c, setting $\partial H(g_c)/\partial g_c = 0$ and solving for g_c results in:

$$\frac{\partial H(g_c)}{\partial g_c} = \frac{1}{2}\left[(a_2 + c_a)\left(\frac{g_{eff}}{g_c}\right)^2 + \frac{\left(\frac{g_{eff}}{g_c}\right)^2 a_1\left(c_a - 2c_p - a_2\right) - g_{eff}\left(\frac{g_{eff}}{g_c}\right)^2 (a_2 + c_a)^2}{\sqrt{\gamma_a}}\right] - 1.6\lambda \mathrm{VPD_L} = 0. \tag{10}$$

$$g_c = \frac{a_1 g_m}{a_1 + g_m(a_2 + sc_a)}\left(\sqrt{\frac{c_a - c_p}{1.6\,\lambda \mathrm{VPD_L}} - 1}\right). \quad (15)$$

Combining equations (3), (13) and (15), an expression for A as a function of g_c is given as:

$$A = g_c\sqrt{1.6\,\lambda \mathrm{VPD_L}(c_a - c_p)}. \quad (16)$$

Hereafter, the result in equation (16) is referred to as the linear optimization model. The g_m is one of the key factors in the non-linear and linear optimization models. This study also provides a mechanism to model g_m, which constitutes one of the main results of the work here.

When g_m is not directly measured, a stress function between c_c and c_i is now proposed to estimate g_m, and is given by

$$\frac{c_c - c_{cmin}}{c_i} = r \approx r_{max}\left[1 - \left(\frac{\mathrm{EC_{dw}}}{\mathrm{EC_{dw\ max}}}\right)^2\right] = r_{max}\left[1 - \left(\frac{\psi_L}{\psi_{L\,max}}\right)^2\right], \quad (17)$$

and

$$g_m = \frac{A}{(1-r)c_i - c_{cmin}} \quad (18)$$

where ψ_{Lmax} is the maximum leaf water potential, $EC_{dw\ max}$ is the maximum electrical conductivity of drainage water, which reflects the level of drainage water salinity that would lead to no appreciable yield (or $A = 0$). Based on a threshold-slope linear salinity response model (Maas and Hoffman, 1977), the calculated $EC_{dw\ max}$ was ~ 43 dS m^{-1} determined from an expansive data set described elsewhere (Qiu *et al.*, 2017b). However, a theoretical $EC_{dw\ max}$ may be deemed infinite if a sigmoidal-shape salinity response model is adopted (Van Genuchten and Hoffman, 1984). As a compromise between these two end-members, the $EC_{dw\ max}$ was set to 60 dS m^{-1} here, where the relative yield (or A) was reduced to 20% in a sigmoidal-shaped model.

The r_{max} and c_{cmin} are the maximum ratio and minimum c_c, respectively, estimated from the measured A–c_i curves under Rubisco limitations. Alternatively, this c_{cmin} can be estimated from the linearized Farquhar biochemical demand model as $c_{cmin} = c_p - rc_p^*$, where c_p^* is a proxy for the c_i compensation point. From equation (1), below c_p, $A < 0$, thus $c_c > c_i$ and $c_p^* < c_p$. In fact, these two parameters have the following relation (Flexas *et al.*, 2007): $c_p^* = c_p - R_d/g_m$. Combining these two equations results in:

$$c_{cmin} = (1-r)c_p + r\frac{R_d}{g_m} \quad (19)$$

The evaluation of this result (i.e. equation 19) is featured in the Discussion section.

In equation (17), the use of leaf water potential instead of EC_{dw} is preferred because EC_{dw} is an indirect measure of leaf water status. Because the leaf water potential was not measured, an equilibrium approximation between salinity concentration in the leaf and the soil must be adopted to proceed further. It is assumed that when salinity in the drainage water is proportional to salinity concentration in the leaf (as common when using filtration theory with constant filtration efficiency), then EC_{dw} describes the expected osmotic potential in the leaf. Evidence and plausibility arguments for the link between EC_{dw} and leaf water status are described elsewhere (Perri *et al.*, 2018). The mathematical form of expressions (17) and (18) and its justification when stomata are not the only limiting factor has been the subject of a recent investigation described elsewhere (Dewar *et al.*, 2018).

Salinity effect on g_m, V_{cmax}, J_{max} and λ

From measured A–c_i curves on hot pepper seedlings, g_m, V_{cmax}, J_{max} and c_c were determined using a non-linear regression method with matlab software for different irrigation water salinity (EC_{iw}) levels. Generally, estimated g_m, V_{cmax}, J_{max} decreased as the electrical conductivity of drainage water (EC_{dw}) increased some 27 days after transplanting (DAT; Figure 1a–c). The g_m, V_{cmax}, J_{max} at EC_{dw} of 7.3 dS m^{-1} decreased by 41.2%, 38.7%, 31.2%, respectively, compared with EC_{dw} at 0.9 dS m^{-1}. The salinity stress has little impact on the relation between c_c and c_i derived for 27 DAT. The c_c increased linearly as c_i increased based on the pooled data from all treatments (Figure 1d). Independent data from other experiments conducted for bell pepper and greenhouse experiments for hot pepper without salinity or water stress are included in Figure 1(d) for reference. All in all, the agreement between these published data sets and the inferred $c_c - c_i$ relation determined from non-linear regression here is acceptable, and suggests that the derived relation in Figure 1(d) is robust and widely applicable to other crops. The estimated r_{max} and c_{cmin} for pepper were 0.49 and 37 μmol mol^{-1}, respectively, from all data sets (Figure 1d), which were then used when analyzing the gas exchange data set in equations (17) and (18) at ambient (c_a).

For the gas exchange data set, the g_m and V_{cmax} estimated based on equation (18) and the non-linear optimization model, respectively, also exhibited a decreasing trend with increasing EC_{dw} from 2.4 dS m^{-1} sampled 23 DAT (Figure 2a,b). These findings are consistent with the result from the independently measured A–c_i curves earlier discussed. The different values of estimated g_m and V_{cmax} between A–c_i curve experiments (described later) and the gas exchange data set are due to leaf temperature (T_L) differences. The V_{cmax} exponentially increases with increasing T_L (the equation is shown in Table S1). The g_m showed a similar trend as V_{cmax} with a certain range of T_L, but decreased at high T_L

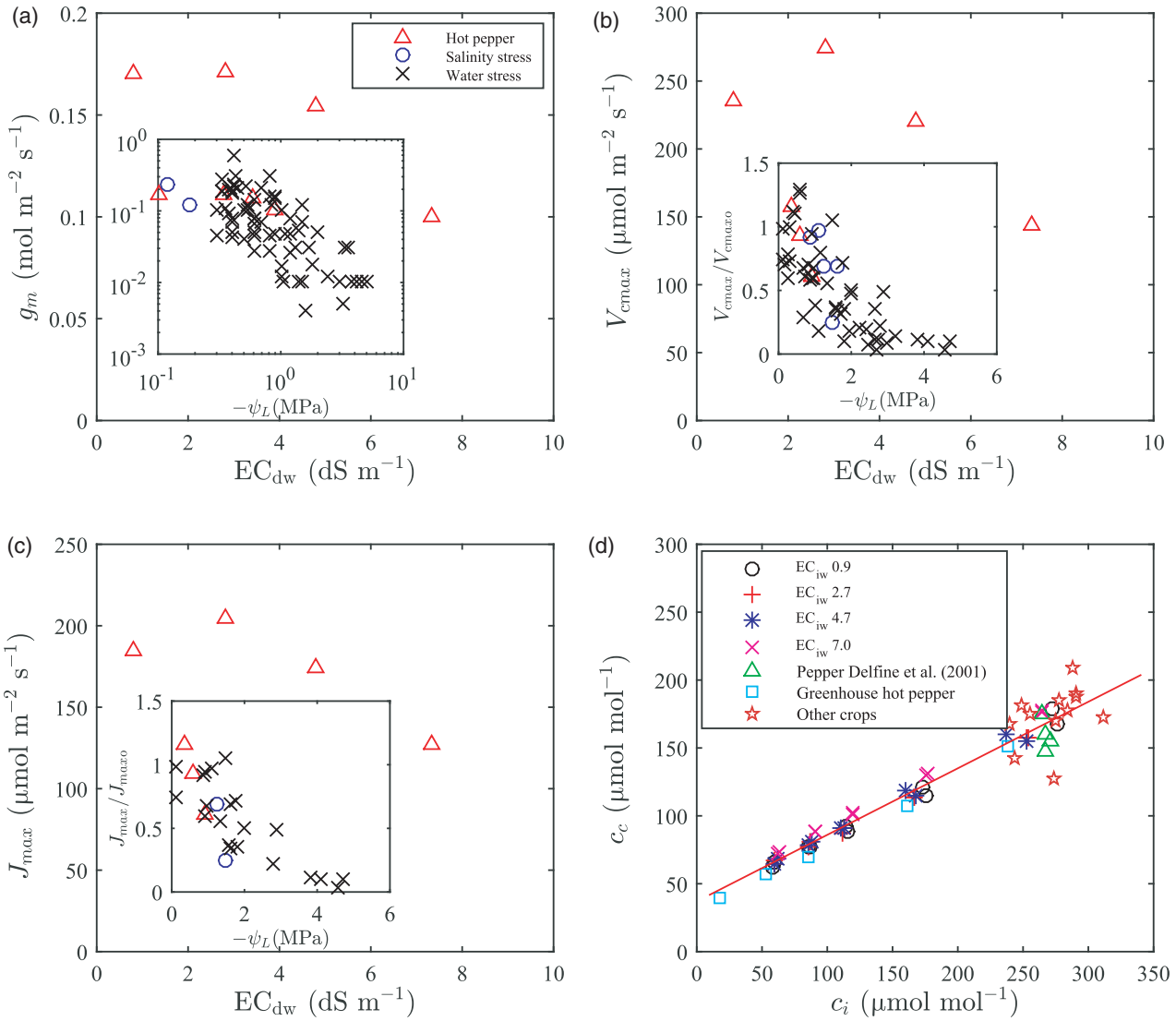

Figure 1. Effects of drainage water salinity (EC_{dw}) on estimated (a) mesophyll conductance (g_m), (b) maximum carboxylation capacity of Rubisco (V_{cmax}), (c) maximum electron transport rate (J_{max}), and (d) relation between chloroplast CO_2 (c_c) and intercellular CO_2 concentration (c_i) for Rubisco limitation from A–c_i curves measured 27 days after transplanting (DAT). For reference, the gas exchange data with no water, salinity and nitrogen stresses from Delfine *et al.* (2001) for bell pepper, from a greenhouse experiment for hot pepper in 2008–2009 (A–c_i curve, not published) and from data for other crops are shown in (d). The regression function for peppers in (d) was with a coefficient of determination R^2 = 0.97. The data in the insets of (a), (b) and (c) are mainly derived from a large number of experiments on drought stress where leaf water pressure was reduced due to soil moisture reductions. Some salt stress experiments have been reported and included as well in the insets (Data S1). Note the collapse of the data sets despite the differing measuring methods, crop type and replication.

(Sharkey *et al.*, 2007). The r value calculated from equation (17) showed minor reduction (from 0.49 to 0.48) as EC_{dw} increased from 1.0 to 6.4 dS m^{-1} (Figure 2c), which is in line with the result from the independent A–c_i curves (Figure 1d). The mean values of λ_{LI} (inferred from the linear optimization model) and λ_{NL} (inferred from the non-linear optimization model) of individual leaves for each salinity level are shown in Figure 2(d). λ_{LI} and λ_{NL} increase almost linearly with increased EC_{dw}, suggesting that the cost per unit mass of water transpired increased linearly as salinity increased. There is a significant correlation between λ_{LI} and λ_{NL} (coefficient of determination R^2 = 0.99 based on the pooled data from all gas exchange data sets). The linear optimization model only underestimated λ_{NL} by about 2.6%, indicating that λ_{LI} can still provide acceptable estimates of λ for operational purposes or parameter constraints.

Effects of elevated CO_2 and salinity on gas exchange

The results from the linearized optimization model are now used to assess how much elevated c_a is required to buffer plants against salinity in the foreseeable future. For this purpose, all EC_{iw} levels were considered along with the

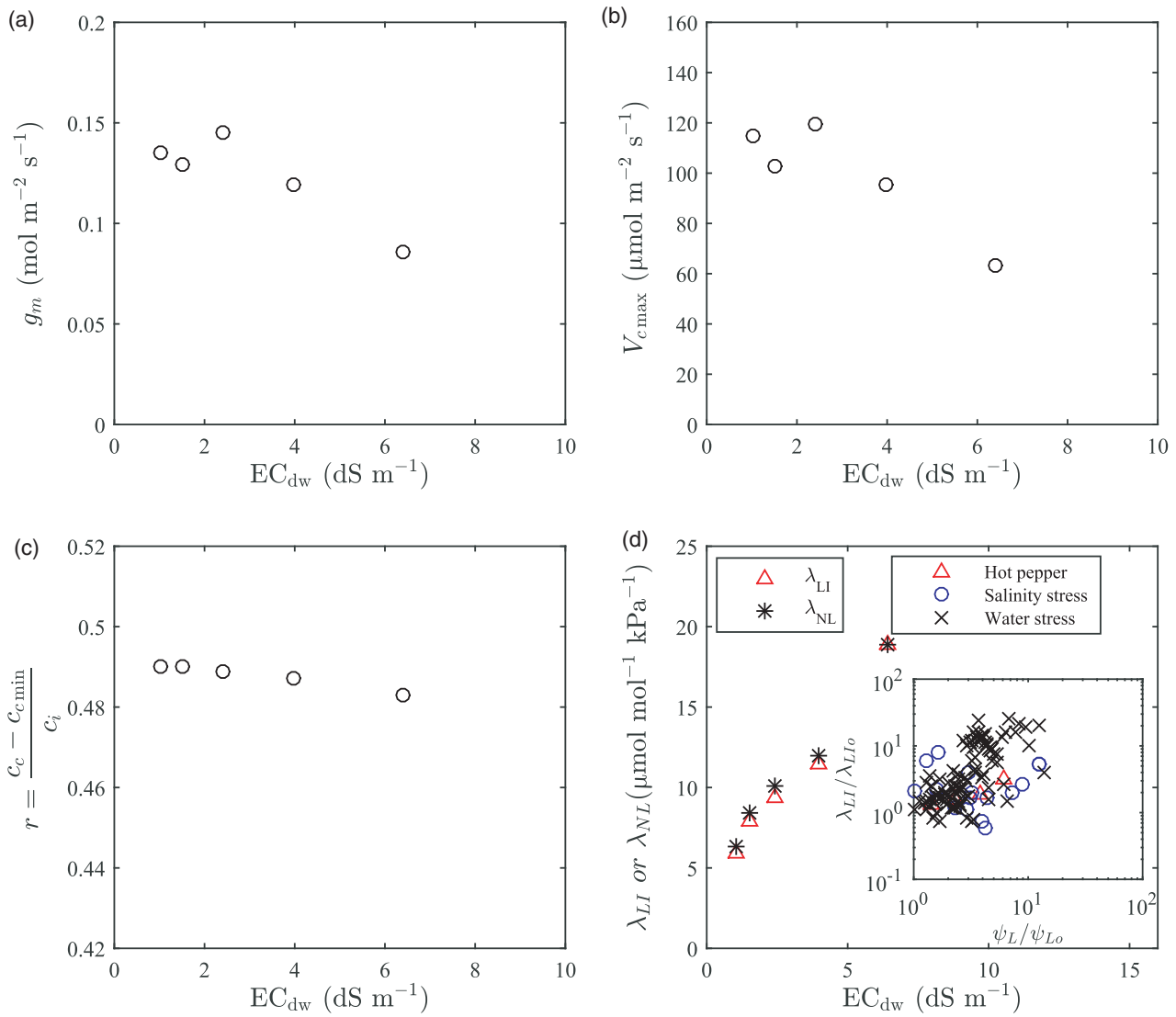

Figure 2. Effects of drainage water salinity (EC_{dw}) on estimated (a) mesophyll conductance (g_m), (b) maximum carboxylation capacity of Rubisco (V_{cmax}), (c) r and (d) marginal water use efficiency estimated from a linear (λ_{LI}) and a non-linear (λ_{NL}) optimization model for g_c. The data were from gas exchange measurements 23 days after transplanting (DAT). The inset in (d) includes data from drought stress studies described in Data S1.

values of kinetic constant for photosynthesis ($a_1 = V_{cmax}$, J_{max}) and g_m estimated from 23 DAT. The premise here is that a_1 and g_m values are not altered by elevated c_a (Katul *et al.*, 2010; Volpe *et al.*, 2011). This assumption is likely to be an overestimate for the effects of elevated c_a on A as downregulation can reduce a_1 with increasing c_a. Long-term exposure to CO_2 enrichment plants may also adjust their morphology, which is not considered here. The value of parameter s (long-term c_c/c_a) used in the linearized optimization model [equations (11)–(15)] was calculated from the long-term c_i/c_a and $(c_c-37)/c_i = 0.49$ derived from the A–c_c curve, and this ratio is assumed to be not sensitive to c_a. The elevated c_a (from 360 to 500 μmol mol^{-1}) has a minor impact on s in the linear model. To simplify, the c_a was set to 430 μmol mol^{-1} when evaluating s values (i.e. 0.483, 0.483, 0.478, 0.474 and 0.459, respectively, for different EC_{iw} levels). The mean values of measured VPD_L were used in all calculations because salinity had little effect on VPD_L (10% variation among treatments). The dependence of λ_{LI} on c_a was assumed linear for Rubisco limited photosynthesis as discussed elsewhere (Katul *et al.*, 2010; Manzoni *et al.*, 2011; Volpe *et al.*, 2011; Vico *et al.*, 2013), and was given by: $\lambda_{LI} = \lambda_{LI0}\frac{c_a - c_p}{c_{a0} - c_p}$, where c_{a0} = 360 μmol mol^{-1}. The compensation point, c_p, is defined as the concentration when $A = 0$ [equation (16)]. The values of λ_{LI0} estimated from 23 DAT for different EC_{iw} levels were used to calculate the effects of elevated c_a on λ_{LI}.

The modeled A increased linearly with elevated c_a for all EC_{iw} levels (Figure 3a), partially offsetting the adverse impacts of salinity stress. The slope of the linear relation between A and c_a decreased as EC_{iw} levels increased. That is, the gains in A with increasing c_a are ameliorated by increased salinity. In fact, an increase of 1.4-fold c_a for EC_{iw} of 7.0 dS m^{-1} can only attain ~ 57% of the same value of A as under EC_{iw} of 0.9 dS m^{-1} in ambient CO_2. However, at low salinity levels, future increases in c_a may offset the short-term osmotic effects of salinity on A. Interestingly, the g_c, c_c/c_a and E are all mildly reduced as c_a and EC_{iw} increased (Figure 3b–d). However, the reductions in g_c, c_c–c_a and E with increasing c_a are minor and are only 3.4%, 2.1–4.5% and 3.4%, respectively, when c_a increased by as much as 40%.

DISCUSSION

New experiments on leaf-gas exchange from hot pepper seedlings were conducted and interpreted using a model for stomatal adjustment based on optimization principles described in Results. This combination of data and model results allows for the evaluation of the relative impairment of photosynthetic and hydraulic machinery of leaves with increased salinity. In this interpretation, photosynthetic properties were represented by g_m and a_1, while hydraulic properties were represented by the marginal water use efficiency λ (Volpe *et al.*, 2011).

Estimated g_m from A–c_i curves measurements decreased with increasing salinity after a moderate salinity level was crossed. Similar results were reported for *Spinacia*

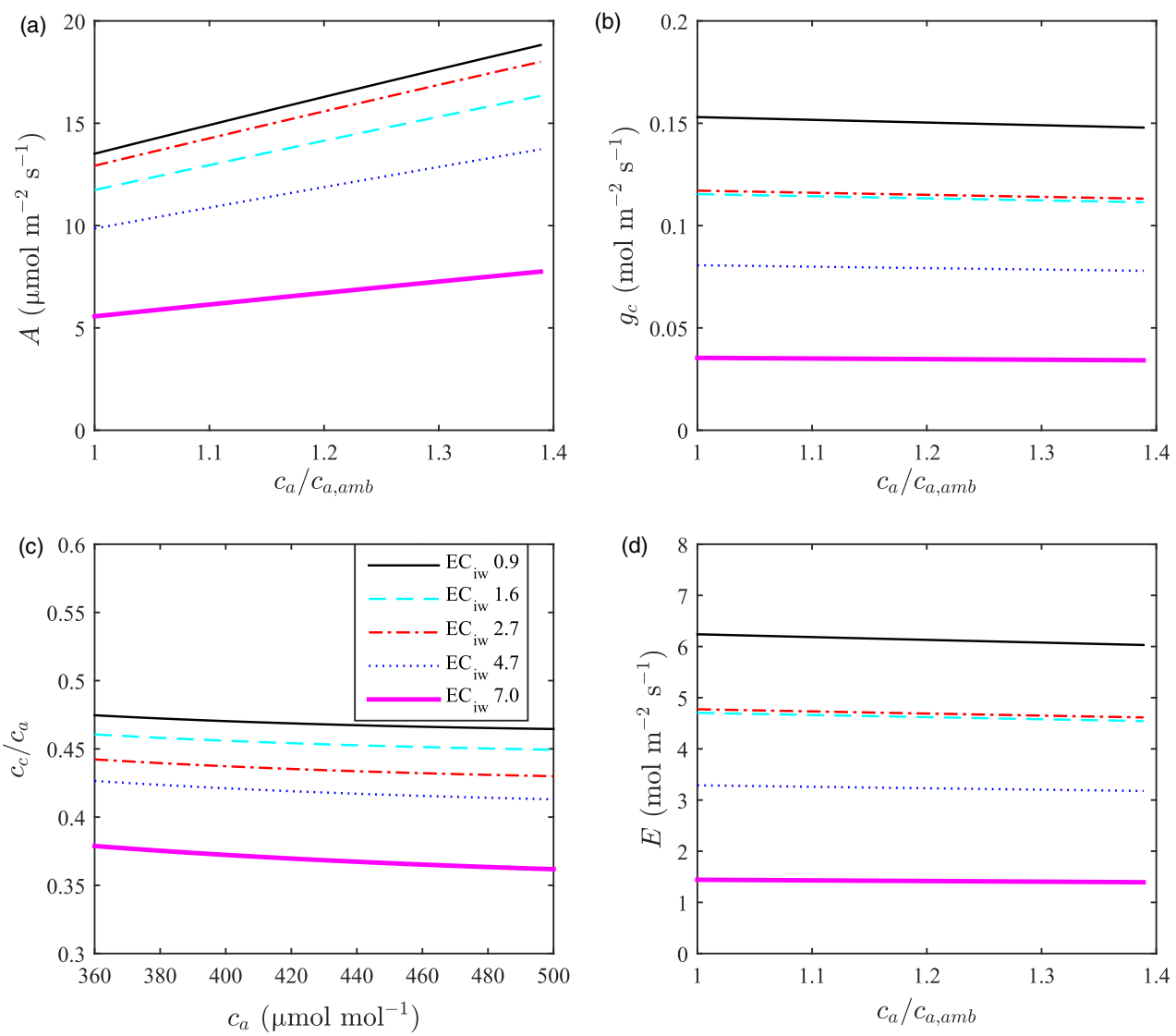

Figure 3. Effects of elevated CO_2 concentration (c_a) on modeled (a) photosynthetic rate (A), (b) stomatal conductance (g_c), (c) relation between c_c/c_a and c_a and (d) leaf transpiration rate (E) under different irrigation salinity levels (EC_{iw}). The ambient CO_2 is set to 360 μmol mol^{-1}.

oleracea (intermediate salt tolerance) and *Olea europaea* (mild salt tolerance; Delfine *et al.*, 1998, 1999; Centritto *et al.*, 2003; Loreto *et al.*, 2003). The modeled g_m from gas exchange measurements using the proposed equation (18) here captured the trends in the aforementioned studies. Based on literature survey, there are three methods to estimate g_m, i.e. gas exchange and chlorophyll fluorescence method, carbon isotope discrimination method and curve fitting method (Flexas *et al.*, 2007, 2008). Only the curve fitting method was used here with limited replications of the A–c_i curve for each EC_{iw} level. However, the limited replication for each EC_{iw} was necessary to ensure a wide range of EC_{iw} values. Nonetheless, the limited replications of the A–c_i cannot preclude some bias in the estimation of g_m. Notwithstanding this replication issue, the overall results for pepper seedlings here are shown to be consistent with many other studies on other crops (see literature review) where g_m was determined by the other two methods, lending some confidence to the robustness of the results here.

A model-data finding is a connection between r and c_{cmin} derived from the relation between c_c and c_i [equation (17); Figure 1d], which is an expansion of a previous model presented in Volpe *et al.* (2011). A similar mathematical form of equation (17) was recently reported, where linear reduction of $(c_c - c_p)/(c_i - c_p)$ was defined as ψ_L increased (Dewar *et al.*, 2018). In equation (17), the r value was affected by two factors. The first is the value of $EC_{dw\,max}$ (or ψ_{Lmax}), which affects the gradient of g_m induced by salinity (or ψ_L). The second is the r_{max}, which affect the initial value of g_m. Higher r_{max} results in higher g_m. From the linear correlation between c_c and c_i found here, the intercept can be obtained and appropriately labeled as c_{cmin} (obtained when $c_i = 0$). Equation (1) suggests that there should be a concentration gradient between c_c and c_i whenever a steady-state CO_2 flux through the leaf is established (Ethier and Livingston, 2004). That is, any c_c should be higher than c_{cmin} because $c_i > 0$ and $c_c > c_i > 0$ from equation (1) when $A < 0$ and $c_a \geq 0$. This c_{cmin} could also be derived with aforementioned equation (19). Upon pooling data for all A–c_i curves, the average T_L was 32.3°C resulting in an average c_p of 47 μmol mol^{-1}. The average values of R_d and g_m were 4 μmol m^{-2} sec^{-1} and 0.15 mol m^{-2} sec^{-1}, respectively. Using these data together with $r = r_{max} = 0.49$, the calculated c_{cmin} from equation (19) was 37 μmol mol^{-1}. This value is in agreement with the value obtained from the correlation between c_c and c_i. For different crops, the values of c_{cmin} and r_{max} may be varied, but their relation is similar to the one shown here. For instance, assuming the same c_{cmin} of 37 μmol mol^{-1}, the calculated r_{max} varied from 0.42 to 0.60 for no stress plants, where data for c_c and c_i are shown in Figure 1(d). The minor change in the value of r in this study indicated that the reduction of c_c and c_i is nearly synchronous for young leaves of hot pepper, and the reduction of g_m is mainly due to the faster reduction in A than c_i [equation (18)]. However, several studies show that lower ψ_L did induce a lower value of c_c than c_i under drought experiments, in turn leading to lower r (Warren *et al.*, 2004; Delfine *et al.*, 2005).

The reductions in g_m and g_c for higher salinity lead to a lower c_c (see Figure 3c at ambient c_a), which limited A (Delfine *et al.*, 1998; Loreto *et al.*, 2003). Except for those inhibitions of CO_2 diffusion (linked to g_m and g_c), the photosynthetic capacity of leaves, a_1, decreased after a moderate salinity level is crossed, which also caused a reduction in A.

The hydraulic properties encoded by λ, calculated from linear and non-linear optimization models both increased with increased salinity. Recalling that $\lambda_{LI} \sim (WUE_{int})^2$ [reversing equation (16) and assuming VPD_L is not significantly affected by salinity (supported by the data here)], the increase in λ as salinity increased is not surprising given the definition of intrinsic water use efficiency $WUE_{int} = A/g_c$. A high WUE_{int} in high salinity is expected because g_c is reduced faster than A as salinity increased, a known result supported by many experiments (Chartzoulakis and Klapaki, 2000; Azuma *et al.*, 2010; Fernández-García *et al.*, 2014). This severe reduction in g_c and corresponding E reduces salt loading into leaves and avoids irreversible (or plastic) damage (Koyro, 2006; Volpe *et al.*, 2011) commonly associated with ionic stresses. Although λ increased monotonically with increasing salinity within the range of salinity levels considered here (corresponding to linear increased WUE_{int}), additional data on more severe salinity levels are necessary to evaluate the correlation between λ and salinity. For instance, when recalculating data from Chartzoulakis and Klapaki (2000), there was only a small increase in WUE_{int} when EC_{iw} increased from 12.6 to 17.8 dS m^{-1}, indicating λ did not appreciably increase for the aforementioned study. The correlation between linear and non-linear optimization models shows that λ_{NL} of hot pepper can be approximated by λ_{LI}, which is independent of g_m and can be readily calculated from measured A, g_c and VPD_L [reversing equation (16)]. This correlation is in line with other studies on trees (e.g. *Pinus taeda* and *Pinus sylvestris*) and spinach (*Spinacia oleracea*; Katul *et al.*, 2010; Launiainen *et al.*, 2011; Volpe *et al.*, 2011), although overestimation of λ in the linear optimization model was observed in prior studies.

The g_m, V_{cmax}, J_{max} and λ variations across different salinity levels for hot pepper were compared against values reported across many drought experiments for several crops for varying ψ_L. The overall patterns in g_m reductions and λ increases with decreased ψ_L (whether drought or salinity induced) are broadly comparable (Figures 1 and 2). Likewise, the decrease in computed V_{cmax} and J_{max} with decreased ψ_L (drought or osmotically induced) appear

comparable and are suggestive of photosynthetic impairment (Figure 1). Hence, osmotic (and not ionic) stress is the dominant factor responsible for the adjustments in g_m, λ and photosynthetic capacity. This finding may not be a surprise as ionic stress requires longer salt accumulation duration and may be a factor in adult plants, not the seedlings analyzed here. Many studies also showed that early response to drought and salinity stress has been mostly identical (Munns, 2002; Chaves *et al.*, 2009).

The c_a has increased since the pre-industrial era, and is projected to increase further in the future (Pachauri *et al.*, 2014). Hence, an extension of this study is to assess the combined effects of elevated salinity and c_a on gas exchange of young hot pepper leaves. The linear optimization model is used for illustration, though the findings here also apply for the non-linear optimization model. An assumption that λ linearly increased with increasing c_a was adopted, which is confirmed by prior studies for the case of Rubisco limitation (Katul *et al.*, 2010). Unsurprisingly, salinity stress inhibits A, g_c, E and c_c/c_a (Figure 3 under ambient c_a). The elevated c_a ameliorated the A, but only under low salinity levels. There was a similar positive effect of elevated c_a on A, while negative effects on g_c or E were reported in *O. europaea* (Volpe *et al.*, 2011) and *P. taeda* (Katul *et al.*, 2010) when using $\lambda \propto c_a$. Manzoni *et al.* (2013) also demonstrated an increased A but no reductions in g_c for elevated c_a using a dynamic optimization scheme where transients in soil moisture were considered. The results here suggest that the inhibition of A by salinity stress may be partly buffered by elevated c_a but only for low salinity levels. The model results derived here are intended to serve as conjectures or hypotheses to be tested in future experiments with elevated CO_2 and salinity.

EXPERIMENTAL PROCEDURES

Experiment

The details of the experimental setup are presented elsewhere (Qiu *et al.*, 2017a, 2018). Briefly, the experiment was conducted using pots positioned in a rain shelter at the Agro-Meteorology Research Station located in Nanjing city, China (32.2°N, 118.7°E, altitude 14.4 m). Five irrigation water salinity (EC_{iw}) characterized by electrical conductivity levels (i.e. 0.9, 1.6, 2.7, 4.7 and 7.0 dS m^{-1}) with four replications at a leaching fraction (the fraction of amount of drainage water relative to amount of irrigation water) of 0.29 were used. Irrigation water salinity was increased by adding 1:1 milli equivalent concentrations of NaCl and $CaCl_2$ to fertilizers (a half-strength Hoagland solution; Qiu *et al.,* 2017a), which added an electrical conductivity of 0.9 dS m^{-1} to the irrigation water for each treatment. The hot pepper plants (*Capsicum annum* L., cultivar Bocuiwang) were transplanted on 28 April 2015 with one plant per pot. Saline water treatments commenced 10 days after the transplanting date. For each salinity treatment, two sets of measurements were collected: (i) A–c_i curves were obtained at near constant air temperature by varying c_a; and (ii) gas exchange measurements where c_a was retained at ambient level. The former were primarily used to estimate the photosynthetic properties including g_m and a_1, whereas the latter explored additional effects of salinity on hydraulic properties (mainly λ).

The A–c_i curves

The A–c_i curves for each treatment except for EC_{iw} of 1.6 dS m^{-1} with two replications were measured on 27 DAT (sunny days) using a LI-6400 photosynthesis system with a red and blue light-emitting diode (LED) source over an area of 6 cm^2 (LI-COR, Lincoln, NE, USA). The limited replication was necessary due to the need to sample a wide range in EC_{iw}. During the gas exchange measurements, ambient CO_2 concentrations were set up by decreasing it from 400 to 250, 150, 100 and 50 μmol mol^{-1}, and then increasing it from 500 to 700, 1000 and 1500 μmol mol^{-1} at a fixed photosynthetic photon flux density (PPFD) of 1200 μmol m^{-2} sec^{-1}. The flow rate was set as 500 μmol sec^{-1}. The average T_L, RH and VPD_L among salinity treatments were 32.3 ± 0.45°C, 44.1 ± 1.9% and 2.1 ± 0.21 kPa, respectively, and did not vary appreciably. Ensuring constant environmental conditions for the many salinity levels was another factor necessitating limited replication.

The gas exchange measurement

Leaf gas exchange parameters including A, E, c_i, c_a, g_c and VPD_L were measured between 09:00 and 11:00 hours on 23 DAT (sunny days) using a LI-6400 photosynthesis system with a red–blue LED source (LI-COR). Four fully grown leaves per treatment were measured with a fixed PPFD level of 1200 μmol m^{-2} sec^{-1} (light saturated based on measured light-response curves) at ambient c_a. The flow rate was 500 μmol sec^{-1}. The T_L, RH and VPD_L among salinity treatments were 29.6 ± 0.33°C, 36.8 ± 3.6% and 2.6 ± 0.13 kPa, respectively.

Other measurements

The drainage water from each pot was collected using a glass bottle positioned beneath each pot. The electrical conductivity of the collected drainage water (EC_{dw}) was measured using a dual channel pH/mV/Ion/Conductivity benchtop meter (MP522, Shanghai SanXin Instrumentation, China) after each irrigation event. The values of $\delta^{13}C$ in the leaves in EC_{iw} of 0.9, 4.7 and 7.0 dS m^{-1} were measured using a MAT253 Stable Isotope Ratio Mass Spectrometer (Thermo Fisher Scientific, San Jose, CA, USA) at the end of the experiment, and are presented elsewhere (Qiu *et al.*, 2019). The values of $\delta^{13}C$ in the other two EC_{iw} levels were estimated based on correlation between $\delta^{13}C$ and EC_{iw}. The values of $\delta^{13}C$ were then used to estimate long-term c_i/c_a according to conventional approaches (Farquhar *et al.*, 1989) not repeated here.

Model parameter determination

When varying c_a from 20 to 1500 μmol mol^{-1}, each measured A–c_i curve spans both Rubisco and RuBP limitations (Figure 4). Hence, it is possible to estimate g_m, V_{cmax}, J_{max} and R_d from each A–c_i curve using a non-linear regression method (see Appendix S1 and Table S2 for approach, comparison with other published methods). These inferred parameters can then be related to the salinity levels experienced by the seedling. The basic equations used in parameter inferences were (Sharkey *et al.*, 2007):

$$A = \frac{a_1(c_c - c_p)}{a_2 + c_c} - R_d; c_c = c_i - \frac{A}{g_m}, \tag{20}$$

where A and c_i are measured. When fitting the A–c_i curve, a critical c_i of 300 μmol mol^{-1} was found to separate Rubisco and RuBP

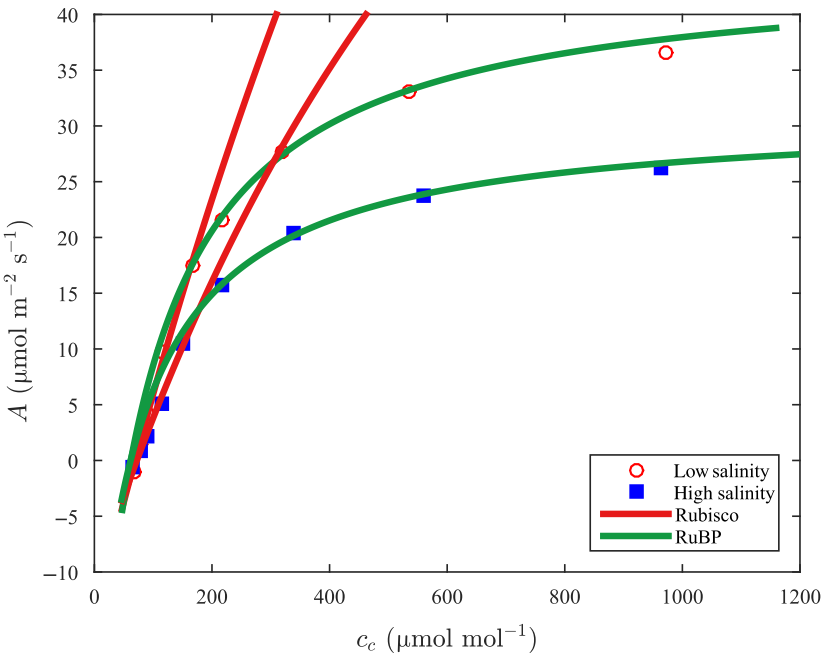

Figure 4. An example of Rubisco and RuBP limited photosynthesis fitted to measured A–c_c curves under different irrigation water salinity levels. The low and high irrigation water salinity levels were 0.9 and 7.0 dS m^{-1}, respectively, used in this study. The photosynthetic rate at any c_c is the minimum of these potential limitations.

limits on A, where Rubisco limits A for $c_i < 300$ μmol mol^{-1}, whereas RuBP limits A for $c_i > 300$ μmol mol^{-1}. However, when measured A variations drop below 2% with increasing c_i, it was assumed that triose phosphate utilization (TPU) limits A (i.e. $\partial A/\partial c_i \approx 0$). TPU limitations occurred at high c_i > 1200 μmol mol^{-1}. The parameters here obtained using matlab software (MathWorks, MA, USA) were then compared with another standard method (made public via a downloadable spreadsheet requiring A–c_i curve) described elsewhere (Sharkey *et al.*, 2007; Table S2), though similar methods are also available (Gu and Sun, 2014; Sun *et al.*, 2014). Deviations among fitted parameters here and the standard approach (Sharkey *et al.*, 2007) were below 10%. The calculations were repeated by commencing the search for optimal parameter combinations using several initial conditions so as to ensure that the search along the parameter manifold is not prematurely terminated at a local minimum for reasons discussed elsewhere (Gu and Sun, 2014). The usage of the proposed non-linear parameter inference method here permits routine analysis of numerous A–c_i curves in a self-consistent manner. The Rubisco limited A in the A–c_i curves (Figure 1) were used to analyze relations between c_c and c_i for different salinity levels.

For the gas exchange data set, c_a did not vary from its ambient value. Optimal g_c in equations (10) and (16) were employed separately. Both formulations require the parameters g_m, a_2, c_p, a_1 and λ. The parameter g_m was estimated from the aforementioned equation (18) with measured A and c_i and estimated r and c_{cmin}. The parameters a_2 and c_p were determined, as before, from temperature adjustment equations (Sharkey *et al.*, 2007) shown in Table S1. The parameter a_1 was estimated by inverting equation (5) with measured A, T_L and estimated c_c from equation (17). The cost parameter λ of individual leaves was determined by inverting equations (10) and (16) for both the non-linear and linear optimization models, respectively.

Literature review

Many studies show that plant response to salinity stress resembles drought stress at the early stages (Munns, 2002; Chaves *et al.*, 2009). Specifically, the early and rapid decline in growth among plants is often linked to osmotic instead of ionic stresses (Perri *et al.*, 2018). Hence, the effects of salt stress on reducing g_m, V_{cmax}, J_{max} and increasing λ here are compared with other salt stress experiments as well as drought experiments on several plant species. Data sets were compiled from the literature that feature reductions in g_m, V_{cmax}, J_{max} and increases in λ relative to a reference unstressed (or well-watered) condition. In drought experiments, changes in g_m, V_{cmax}, J_{max} and λ are presented as a function of reduced plant water potential ψ_L. In the case of salinity stress for well-irrigated crops (as is the case here), the plant water potential was not measured but was inferred as follows. The EC_{dw} was converted to ψ_L assuming: (i) osmotic pressure dominates the overall total water potential (no gravitational or pressure potentials) in the leaf (a reasonable assumption for well-watered short plants); and (ii) a 50% dilution ratio of salt concentration in leaves when compared with the drainage water salinity [a reasonable assumption because electrical conductivity of soil saturated paste extract (EC_e) is ~ $0.5EC_{dw}$ measured at the end of the experiment]. The van't Hoff equation $\pi = M_s RT$ is used to relate osmotic pressure (P_i, in atm) to solute molar concentration (M_s, in mol L^{-1}) and temperature (T, in K), where R is the gas constant (= 0.08206 L atm mol^{-1} K^{-1}). Estimation of M_s from EC measurements of soil salinity is based on the approximate linear expression $M_s = bEC + c$, where b and c are based on instrument calibration. To relate soil salinity to salinity in the leaf needed for, it is assumed that salinity concentration in the leaf is in quasi-equilibrium with salinity concentration in the soil-root system (though the soil and leaf pressures differ). That is, the state of equilibrium is restricted to chemical potentials not mechanical pressures. The linear relation between soil and leaf salinity is

often used in models based on filtration arguments where the filtration efficiency varies linearly with external salinity concentration (for review, see Perri *et al.*, 2018). Continuous monitoring of soil water salinity, which is far more desirable than EC_{dw}, is made difficult because of the intrusive effects of such measurements on the rooting system.

DATA STATEMENT

The data set from the experiment and the literature review are available in Data S1. The matlab code for inferring parameters from A–c_i curve was shared freely in the Github: https://github.com/shuilibite?tab=repositories.

ACKNOWLEDGEMENTS

The authors thank J. Xu, J. Chen, S. Cheng, X. Liu and H. Chen for all their assistance during the field experiments, S. Perri and A. Molini for constructive comments and suggestions. R. Qiu acknowledges the support from the National Natural Science Foundation of China (51509130), the Natural Science Foundation of Jiangsu Province (BK20150908), and the financial support by the Jiangsu Provincial Department of Education for carrying out this research at Duke University. G. Katul acknowledges support from the US National Science Foundation (NSF-AGS-1644382 and NSF-IOS-1754893).

AUTHORS' CONTRIBUTIONS

RQ designed and conducted most of the experiment, analyzed the data and wrote the draft manuscript. GK provided the new insights for the model and markedly improved the manuscript. All authors discussed the results and approved the final version of the manuscript.

CONFLICT OF INTEREST

The authors declare that there are no conflicts of interest.

SUPPORTING INFORMATION

Additional Supporting Information may be found in the online version of this article.

Table S1. The values of scaling constant and activation energy describing the temperature adjustment for Rubisco limited photosynthesis.

Table S2. Comparison of values of V_{cmax}, R_d, J_{max}, g_m and TPU under different irrigation water salinity based on the proposed matlab program here and Sharkey *et al.*'s model.

Appendix S1. Literature used and introduction for Data S1.

Appendix S2. Introduction of matlab program for solving A–c_i curve when g_m was unknown.

Data S1. Data set used for Figures 1 and 2.

REFERENCES

Azuma, R., Ito, N., Nakayama, N., Suwa, R., Nguyen, N.T., Larrinaga-Mayoral, J.A., Esaka, M., Fujiyama, H. and Saneoka, H. (2010) Fruits are more sensitive to salinity than leaves and stems in pepper plants (*Capsicum annuum* L.). *Sci. Hortic.* **125**, 171–178.

Ben-Gal, A., Ityel, E., Dudley, L., Cohen, S., Yermiyahu, U., Presnov, E., Zigmond, L. and Shani, U. (2008) Effect of irrigation water salinity on transpiration and on leaching requirements: A case study for bell peppers. *Agr. Water Manage.* **95**, 587–597.

Bonan, G.B., Williams, M., Fisher, R.A. and Oleson, K.W. (2014) Modeling stomatal conductance in the earth system: linking leaf water-use efficiency and water transport along the soil-plant-atmosphere continuum. *Geosci. Model Dev.* **7**, 2193–2222.

Brugnoli, E. and Lauteri, M. (1991) Effects of salinity on stomatal conductance, photosynthetic capacity, and carbon isotope discrimination of salt-tolerant (*Gossypium hirsutum* L.) and salt-sensitive (*Phaseolus vulgaris* L.) C_3 non-halophytes. *Plant Physiol.* **95**, 628–635.

Centritto, M., Loreto, F. and Chartzoulakis, K. (2003) The use of low [CO_2] to estimate diffusional and non-diffusional limitations of photosynthetic capacity of salt-stressed olive saplings. *Plant Cell Environ.* **26**, 585–594.

Chartzoulakis, K. and Klapaki, G. (2000) Response of two greenhouse pepper hybrids to N_aCl salinity during different growth stages. *Sci. Hortic.* **86**, 247–260.

Chaves, M.M., Flexas, J. and Pinheiro, C. (2009) Photosynthesis under drought and salt stress: regulation mechanisms from whole plant to cell. *Ann. Bot.* **103**, 551–560.

Cowan, I.R. (1978) Stomatal behaviour and environment. *Adv. Bot. Res.* **4**, 117–228.

Cowan, I.R. and Farquhar, G.D. (1977) Stomatal function in relation to leaf metabolism and environment. *Symp. Soc. Exp. Biol.* **31**, 471.

Delfine, S., Alvino, A., Zacchini, M. and Loreto, F. (1998) Consequences of salt stress on conductance to CO_2 diffusion, Rubisco characteristics and anatomy of spinach leaves. *Funct. Plant Biol.* **25**, 395–402.

Delfine, S., Alvino, A., Villani, M.C. and Loreto, F. (1999) Restrictions to carbon dioxide conductance and photosynthesis in spinach leaves recovering from salt stress. *Plant Physiol.* **119**, 1101–1106.

Delfine, S., Loreto, F., Pinelli, P., Tognetti, R. and Alvino, A. (2005) Isoprenoids content and photosynthetic limitations in rosemary and spearmint plants under water stress. *Agr. Ecosyst. Environ.* **106**, 243–252.

Dewar, R., Mauranen, A., Mäkelä, A., Hölttä, T., Medlyn, B. and Vesala, T. (2018) New insights into the covariation of stomatal, mesophyll and hydraulic conductances from optimization models incorporating non-stomatal limitations to photosynthesis. *New Phytol.* **217**, 571–585.

Döll, P. and Siebert, S. (2002) Global modeling of irrigation water requirements. *Water Resour. Res.* **38**, 1–8.

Ethier, G.J. and Livingston, N.J. (2004) On the need to incorporate sensitivity to CO_2 transfer conductance into the Farquhar-von Caemmerer-Berry leaf photosynthesis model. *Plant Cell Environ.* **27**, 137–153.

Farquhar, G.D., Ehleringer, J.R. and Hubick, K.T. (1989) Carbon isotope discrimination and photosynthesis. *Annu. Rev. Plant Biol.* **40**, 503–537.

Fernández-García, N., Olmos, E., Bardisi, E., García-De La Garma, J.U.S., López-Berenguer, C. and Rubio-Asensio, J.E.S. (2014) Intrinsic water use efficiency controls the adaptation to high salinity in a semi-arid adapted plant, henna (*Lawsonia inermis* L.). *J. Plant Physiol.* **171**, 64–75.

Flexas, J., Diazespejo, A., Galmes, J., Kaldenhoff, R., Medrano, H. and Ribascarbo, M. (2007) Rapid variations of mesophyll conductance in response to changes in CO_2 concentration around leaves. *Plant Cell Environ.* **30**, 1284–1298.

Flexas, J., Bota, J., Escalona, J.M., Sampol, B. and Medrano, H. (2002) Effects of drought on photosynthesis in grapevines under field conditions: an evaluation of stomatal and mesophyll limitations. *Funct. Plant Biol.* **29**, 461–471.

Flexas, J., Bota, J., Loreto, F., Cornic, G. and Sharkey, T.D. (2004) Diffusive and metabolic limitations to photosynthesis under drought and salinity in C_3 plants. *Plant Biol.* **6**, 269–279.

Flexas, J., Carbo, M.R., Espejo, A.D., Galmes, J. and Medrano, H. (2008) Mesophyll conductance to CO_2: current knowledge and future prospects. *Plant Cell Environ.* **31**, 602–621.

Flowers, T.J., Troke, P.F. and Yeo, A.R. (1977) The mechanism of salt tolerance in halophytes. *Annu. Rev. Plant Physiol.* **28**, 89–121.

Galmés, J., Medrano, H.O.L. and Flexas, J. (2007) Photosynthetic limitations in response to water stress and recovery in Mediterranean plants with different growth forms. *New Phytol.* **175**, 81–93.

Van Genuchten, M.T. and Hoffman, G.J. (1984) Analysis of crop production. In *Soil Salinity Under Irrigation.* (Shainberg, I. and Shalhevet, J., eds). New York: Springer.

Givnish, T.J. and Vermeij, G.J. (1976) Sizes and shapes of liane leaves. *Am. Nat.* **110**, 743–778.

Gu, L. and Sun, Y. (2014) Artefactual responses of mesophyll conductance to CO_2 and irradiance estimated with the variable J and online isotope discrimination methods. *Plant Cell Environ.* **37**, 1231–1249.

Hari, P., Mäkelä, A., Korpilahti, E. and Holmberg, M. (1986) Optimal control of gas exchange. *Tree Physiol.* **2**, 169–175.

Hossain, M.S. and Dietz, K. (2016) Tuning of redox regulatory mechanisms, reactive oxygen species and redox homeostasis under salinity stress. *Front. Plant Sci.* **7**, 548.

Hsiao, T.C., Acevedo, E., Fereres, E. and Henderson, D.W. (1976) Water stress, growth and osmotic adjustment. *Phil. Trans. R. Soc. B* **273**, 479–500.

Jesus, J.M., Danko, A.S., Fiúza, A. and Borges, M. (2015) Phytoremediation of salt-affected soils: a review of processes, applicability, and the impact of climate change. *Environ. Sci. Pollut. R.* **22**, 6511–6525.

Katul, G.G., Palmroth, S. and Oren, R. (2009) Leaf stomatal responses to vapour pressure deficit under current and CO_2-enriched atmosphere explained by the economics of gas exchange. *Plant Cell Environ.* **32**, 968–979.

Katul, G., Manzoni, S., Palmroth, S. and Oren, R. (2010) A stomatal optimization theory to describe the effects of atmospheric CO_2 on leaf photosynthesis and transpiration. *Ann. Bot.* **105**, 431–442.

Koyro, H. (2006) Effect of salinity on growth, photosynthesis, water relations and solute composition of the potential cash crop halophyte *Plantago coronopus* (L.). *Environ. Exp. Bot.* **56**, 136–146.

Launiainen, S., Katul, G.G., Kolari, P., Vesala, T. and Hari, P. (2011) Empirical and optimal stomatal controls on leaf and ecosystem level CO_2 and H_2O exchange rates. *Agr. Forest Meteorol.* **151**, 1672–1689.

Loreto, F., Centritto, M. and Chartzoulakis, K. (2003) Photosynthetic limitations in olive cultivars with different sensitivity to salt stress. *Plant Cell Environ.* **26**, 595–601.

Lycoskoufis, I.H., Savvas, D. and Mavrogianopoulos, G. (2005) Growth, gas exchange, and nutrient status in pepper (*Capsicum annuum* L.) grown in recirculating nutrient solution as affected by salinity imposed to half of the root system. *Sci. Hortic.* **106**, 147–161.

Maas, E.V. and Hoffman, G.J. (1977) Crop salt tolerance–current assessment. *J. Irrig. Drain. Divis.* **103**, 115–134.

Manzoni, S., Vico, G., Katul, G., Fay, P.A., Polley, W., Palmroth, S. and Porporato, A. (2011) Optimizing stomatal conductance for maximum carbon gain under water stress: a meta-analysis across plant functional types and climates. *Funct. Ecol.* **25**, 456–467.

Manzoni, S., Vico, G., Palmroth, S., Porporato, A. and Katul, G. (2013) Optimization of stomatal conductance for maximum carbon gain under dynamic soil moisture. *Adv. Water Resour.* **62**, 90–105.

Morgan, J.M. (1984) Osmoregulation and water stress in higher plants. *Annu. Rev. Plant Physiol.* **35**, 299–319.

Munns, R. (2002) Comparative physiology of salt and water stress. *Plant Cell Environ.* **25**, 239–250.

Munns, R. and Tester, M. (2008) Mechanisms of salinity tolerance. *Annu. Rev. Plant Biol.* **59**, 651–681.

Nadal, M. and Flexas, J. (2018) Chapter 17 – mesophyll conductance to CO_2 diffusion: effects of drought and opportunities for improvement. In *Water Scarcity and Sustainable Agriculture in Semiarid Environment* (García Tejero, I.F. and Durán Zuazo, V.H. eds). London: Elsevier, pp. 403–438.

Pachauri, R.K., Allen, M.R., Barros, V.R., Broome, J., Cramer, W., Christ, R., Church, J.A., Clarke, L., Dahe, Q. and Dasgupta, P. (2014) Climate change 2014: synthesis report. Contribution of Working Groups I, II and III to the fifth assessment report of the Intergovernmental Panel on Climate Change: IPCC.

Perri, S., Entekhabi, D. and Molini, A. (2018) Plant osmoregulation as an emergent water-saving adaptation. *Water Resour. Res.* **54**, 2781–2798.

Perri, S., Katul, G.G. and Molini, A. (2019) Xylem-phloem hydraulic coupling explains multiple osmoregulatory responses to salt-stress. *New Phytol.* **224**(2), 644–662. https://doi.org/10.1111/nph.16072.

Qiu, R.J., Liu, C.W., Wang, Z.C., Yang, Z.Q. and Jing, Y.S. (2017a) Effects of irrigation water salinity on evapotranspiration modified by leaching fractions in hot pepper plants. *Sci. Rep.* **7**, 7231.

Qiu, R.J., Jing, Y.S., Liu, C.W., Yang, Z.Q. and Wang, Z.C. (2017b) Response of hot pepper yield, fruit quality, and fruit ion content to irrigation water salinity and leaching fractions. *HortScience*, **52**, 979–985.

Qiu, R.J., Yang, Z.Q., Jing, Y.S., Liu, C.W., Luo, X.S. and Wang, Z.C. (2018) Effects of irrigation water salinity on the growth, gas exchange parameters, and ion concentration of hot pepper plants modified by leaching fractions. *HortScience*, **53**, 1050–1055.

Qiu, R.J., Liu, C.W., Li, F.S., Wang, Z.C., Yang, Z.Q. and Cui, N.B. (2019) An investigation on possible effect of leaching fractions physiological responses of hot pepper plants to irrigation water salinity. *BMC Plant Biol.* **19**, 297.

Runyan, C.W. and D'Odorico, P. (2010) Ecohydrological feedbacks between salt accumulation and vegetation dynamics: role of vegetation-groundwater interactions. *Water Resour. Res.* **46**, W11561.

Sharkey, T.D., Bernacchi, C.J., Farquhar, G.D. and Singsaas, E.L. (2007) Fitting photosynthetic carbon dioxide response curves for C_3 leaves. *Plant Cell Environ.* **30**, 1035–1040.

Singh, R., Jhorar, R.K., van Dam, J.C. and Feddes, R.A. (2006) Distributed ecohydrological modelling to evaluate irrigation system performance in Sirsa district, India II: Impact of viable water management scenarios. *J. Hydrol.* **329**, 714–723.

Steduto, P., Albrizio, R., Giorio, P. and Sorrentino, G. (2000) Gas-exchange response and stomatal and non-stomatal limitations to carbon assimilation of sunflower under salinity. *Environ. Exp. Bot.* **44**, 243–255.

Sun, Y., Gu, L., Dickinson, R.E. *et al.* (2014) Asymmetrical effects of mesophyll conductance on fundamental photosynthetic parameters and their relationships estimated from leaf gas exchange measurements. *Plant Cell Environ.* **37**, 978–994.

Vico, G., Manzoni, S., Palmroth, S., Weih, M. and Katul, G. (2013) A perspective on optimal leaf stomatal conductance under CO_2 and light colimitations. *Agr. Forest Meteorol.* **182**, 191–199.

Volpe, V., Manzoni, S., Marani, M. and Katul, G. (2011) Leaf conductance and carbon gain under salt-stressed conditions. *J. Geophys. Res. Biogeo.* **116**(G4). https://doi.org/10.1029/2011JG001848

Warren, C.R., Livingston, N.J. and Turpin, D.H. (2004) Water stress decreases the transfer conductance of Douglas-fir (*Pseudotsuga menziesii*) seedlings. *Tree Physiol.* **24**, 971–979.